Characterization and Quantification of Curvature using Independent Coordinates Method in the Human Left Ventricle by Magnetic Resonance Imaging to Identify the Morphology Subtype of Hypertrophy Cardiomyopathy*

Liang Zhong[1,2], Xiaodan Zhao[1], Min Wan[3], Jun-Mei Zhang[1], Bo Yang Su[1], Hak Chiaw Tang[1] and Ru San Tan[1,2]

***Abstract*— The patterns of ventricular hypertrophy are critical determinants of blood flow and function, but are variable. Therefore, it is clinically relevant to assess the hypertrophic shape patterns to better characterize and identify the morphological subtypes. We proposed and developed an independent coordinates method (ICM) to quantify the regional shape of the left ventricle in terms of curvature. 19 normal subjects and 5 HCM (hypertrophic cardiomyopathy) patients with different morphological subtype (i.e., septal hypertrophy, mid-ventricular hypertrophy, reverse curvature septum hypertrophy and sigmoid septum hypertrophy) were recruited and underwent magnetic resonance scans. The curvature along the endocardial and epicardial surface was computed using ICM method and was compared in HCM patients against normal subjects. The results showed that curvature plots are variable in different morphological subtype. The curvature pattern demonstrated the utilities in delineating different subtype. In conclusion, ICM method to quantify regional curvature of the left ventricle from magnetic resonance imaging are feasible in normal subjects and those with hypertrophy cardiomyopathy, which may serve as a novel approach to depict local shape of the left ventricle and to assess the morphological subtype in clinical practice.**

I. INTRODUCTION

Hypertrophic cardiomyopathy (HCM) is a primary disease of the myocardium in which a portion of the myocardium is hypertrophied without any obvious cause. It is the most common inherited cardiac disorders, with an estimated prevalence of 1:500 ([1]-[5]), and the annual mortality is estimated at 1-2%. HCM is characterized by left ventricular hypertrophy with occasional involvement of the right ventricle. The mode of inheritance is autosomal dominant in approximately 50-60% of the cases. There are now more than 10 genes with likely hundreds of mutation (keep going up) ([6]). Depending on whether the distortion of normal heart anatomy causes an obstruction of the outflow of blood from the left ventricle of the heart, HCM can be divided into two types, a more common, obstructive type (HOCM, 70%) and a less common, non-obstructive type (HNCM). In HOCM, the patients symptoms and the obstructive gradient are the guide to treatment.

Magnetic resonance image (MRI) has proven to be an important tool for the evaluation of patients suspected of having HCM because it can readily diagnose those with phenotypic expression of the disorder and can potentially identify the subset of patients at risk of sudden cardiac death ([5]). But we currently lack a quantitative measure that can capture complex left ventricular conformational data, and yet is easily computed and clinical meaningful.

II. CURVATURE DEFINITIONS AND COMPUTATION

In this paper, we assume the planar curve has the representation $\boldsymbol{\alpha}(t) = (x(t), y(t))$, where $x(t), y(t)$ are coordinates and are expressed as functions of the variable t. When t takes some value t_k, $1 \leq k \leq n$, the corresponding discrete points $\{\boldsymbol{p}_k = (x(t_k), y(t_k)) | 1 \leq k \leq n\}$ form the discrete curve $\boldsymbol{\alpha}_d$. The curvature $\kappa(t_k)$ at the point $\boldsymbol{p}_k$ is a measure of how sensitive its unit tangent vector is moving from itself to the neighboring point. If the unit tangent rotates counterclockwise, then $\kappa(t_k) > 0$; otherwise, $\kappa(t_k) < 0$.

A. Definitions of curvature

One definition of curvature at $\boldsymbol{p}_k$ is that the absolute value of $\kappa(t_k)$ equals to the reciprocal of the radius $\rho(t_k)$ of the osculating circle at this point, i.e.,

$$|\kappa(t_k)| = 1/\rho(t_k), \tag{1}$$

but we need to determine the curvature sign at each point. The curvature also has expression with signs:

$$\kappa(t_k) = \frac{x'(t_k)y''(t_k) - y'(t_k)x''(t_k)}{\left(x'(t_k)^2 + y'(t_k)^2\right)^{3/2}}, \tag{2}$$

where $x'(t_k)$ (resp. $x''(t_k)$) is the value of $x'(t)$ (resp. $x''(t)$) at $t = t_k$, and $'$ (resp. $''$) denotes the first (resp. second) order derivative with respect to t, similarly for $y'(t_k)$ and $y''(t_k)$. For curve with analytic representation, we can compute the curvature just using the formula (2). However, for discrete

*Research supported by the National Research Foundation (NMRC/EDG/1037/2011), SingHealth (SHF/FG453P/2011) and (SHF/FG503P/2012), Goh Cardiovascular Research Grant (Duke-NUS-GCR/2013/0009), NHCS Centre Grant Seed Funding (NHCS-CGSF/2014/003), and Singapore-China Joint Research Programme (1215c013).

[1]L. Zhong, et al. are with National Heart Centre Singapore, 5 Hospital Drive, 169609, Singapore. {zhong.liang, zhao.xiaodan, zhang.junmei, su.boyang, tang.hak.chiaw, tan.ru.san}@nhcs.com.sg

[2]L. Zhong, et al. are with Duke-NUS Graduate Medical School, 8 College Road, 169857, Singapore.

[3]M. Wan is with Institute of High Performance Computing, 1 Fusionopolis Way, #16-16 Connexis, 138632, Singapore. wanm@ihpc.a-star.edu.sg

978-1-4244-7929-0/14/$26.00 ©2014 IEEE

curve $\boldsymbol{\alpha}_d$, we do not have expressions for $x(t)$ and $y(t)$. In general, there are two ways to compute curvature for discrete curve. One is analytic curve method, which fits an analytic curve to the local discrete points and computes the curvature by using the analytic definitions, and the other one is discrete structure method. In this paper, we adopt an analytic method–independent coordinates method (see, Lewiner et al. [8]) to compute the curvature.

B. Independent coordinates method (ICM)

Suppose now we have a series of discrete points $\{\boldsymbol{p}_k = (x(s_k), y(s_k))|1 \le k \le n\}$. The curvature at $\boldsymbol{p}_k$ is computed in its sliding window $\{\boldsymbol{p}_i|k-q \le i \le k+q\}$ (q is called the width of the sliding window) by locally fitting a parametric curve $(\hat{x}(s), \hat{y}(s))$ to the discrete curve with

$$\begin{cases} \hat{x}(s) = x(s_k) + x'(s_k)\cdot s + \frac{1}{2}x''(s_k)\cdot s^2; \\ \hat{y}(s) = y(s_k) + y'(s_k)\cdot s + \frac{1}{2}y''(s_k)\cdot s^2, \end{cases}$$

where s is the arc length parameter. The derivatives $x'(s_k)$, $y'(s_k)$, $x''(s_k)$ and $y''(s_k)$ are solved out by two minimization problems, and then the curvature at $\boldsymbol{p}_k$ is computed by using (2),

$$\kappa(s_k) = (eh - fg)/(ac - b^2), \tag{3}$$

where

$$a = \sum_{i=k-q}^{k+q} \omega_i^2(\bar{l}_i)^2;\ b = \sum_{i=k-q}^{k+q} \frac{\omega_i^2}{2}(\bar{l}_i)^3;\ c = \sum_{i=k-q}^{k+q} \frac{\omega_i^2}{4}(\bar{l}_i)^4;$$

$$e = \sum_{i=k-q}^{k+q} \omega_i^2\bar{l}_i(x_i - x_k);\ \ f = \frac{1}{2}\sum_{i=k-q}^{k+q} \omega_i^2(\bar{l}_i)^2(x_i - x_k);$$

$$g = \sum_{i=k-q}^{k+q} \omega_i^2\bar{l}_i(y_i - y_k);\ \ h = \frac{1}{2}\sum_{i=k-q}^{k+q} \omega_i^2(\bar{l}_i)^2(y_i - y_k).$$

Here, $x_i := x(s_i), y_i := y(s_i)$, $\bar{l}_i = l_i - l_k$ with $l_k = \sum_{j=1}^{k-1}[(x_{j+1} - x_j)^2 + (y_{j+1} - y_j)^2]^{1/2}$, and $\omega_i > 0$ is the weight. In the implementation, we choose $\omega_i = 1$. For the points near boundary, its sliding window may not be centered around $\boldsymbol{p}_k$, in this case, we could reduce q or simply use a non-centered window to compute the curvature. The convergence analysis and experimental results in [8] have shown the accuracy and robust of this method.

III. Implementation Procedure

The orientation of endocardium is from mitral valve to aortic valve, and the orientation of epicardium goes in the same direction. In Fig. 1, we display the delineated contours of the endocardium and epicardium at the end-diastolic phase in a two-dimensional cine MR image (left), and the corresponding contour plot in MATLAB (right).

A. Curve smoothing

Next, we adopt high order orthogonal polynomials to smooth the curve. We first find the degree for polynomial fitting, and then compute the fitting orthogonal polynomial at our interesting points (see polydeg.m and orthofit.m from the websit http://www.biomecardio.com/matlab).

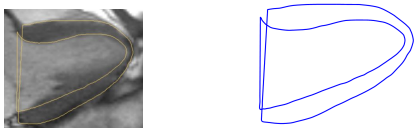

Fig. 1. Left: segmented endocardium and epicardium of two-dimensional cine MR image at end-diastolic phase; Right: discrete contours of endocardium and epicardium output from MATLAB.

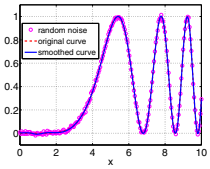

Fig. 2. An example of smoothing noise. We add random Gaussian noise with mean 0 and standard derivation 0.01 to the curve $y = \sin^2(x^3/100), x \in [0, 10]$. We can visually see that the smoothed curve virtually overlaps the original curve.

B. Computation procedure

We assume that all the discrete contours are uniformly sampled in $[0, 1]$. Our computation step for the closed curve containing endocardium is as follows:

- use piecewise cubic spline interpolation to obtain the values at the uniformly sampled points $\{t_k\}_{k=1}^n$ in $[0, 1]$;
- adopt the definition in (1) to roughly compute the curvature for the closed contour containing endocardium, and then use the fact that the curvature of straight line is 0 to find the curve connecting mitral valve and aortic valve. Here, we use the area formula (Heron's formula) to compute $\rho(t_k)$, which is the radius of the circle circumscribed to a triangle formed by the three points $\boldsymbol{p}_{k-1}, \boldsymbol{p}_k, \boldsymbol{p}_{k+1}$, and this leads to
$$|\kappa_d(t_k)| = 4\sqrt{S(S-a)(S-b)(S-c)}/(abc),$$
where $a = \|\boldsymbol{p}_k\boldsymbol{p}_{k+1}\|$, $b = \|\boldsymbol{p}_{k-1}\boldsymbol{p}_{k+1}\|$, $c = \|\boldsymbol{p}_{k-1}\boldsymbol{p}_k\|$ and $S = (a+b+c)/2$.
- smooth the curve connecting mitral valve and aortic valve by the smoothing technique in Subsection III-A;
- adopt the independent coordinates method with n points to compute the curvature for endocardium.
- repeat the above four steps for the closed curve containing epicardium.

IV. Results and Discussions

A. Clinical results

We repeat the five steps in Subsection III-B to the end-diastolic (ED) and end-systolic (ES) phases of our nineteen normal subjects and five HCM patients. For comparison consistency, we add a minus sign to the computed curvature when the curve rotates clockwise.

In the computation, we take the number of points $n = 600$, and the width of the sliding window $q = 3$. In Fig. 3-Fig. 7, the order of subfigures is as follows:

- The first row: segmented endocardium and epicardium of two-dimensional cine MR images at ED (left) and ES (right) phases;

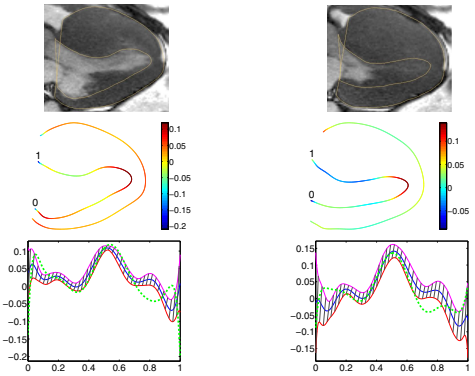

Fig. 3. Septal hypertrophic cardiomyopathy in a 48-year-old man.

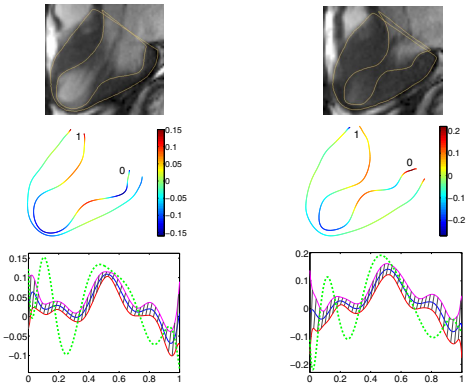

Fig. 4. Mid-ventricular hypertrophic cardiomyopathy with a "burned out apex" in a 41-year-old woman.

- The second row: color-mapping representation of ED (left) and ES (right) phases, i.e., we represent the given location by its corresponding curvature value as the color of the marker. We also mark the starting point–mitral valve ("0") and the ending point–aortic valve ("1") in the subfigures.
- The last row: the banded area is the mean (middle blue line) and mean±SD (standard derivation) of the subjects, and the green dash line is the endocardium curvature plot of HCM patient (left: ED phase; right: ES phase). Note that we have added a minus sign if the curve rotates clockwise.

We analyze the hypertrophic myocardium for each patient in the caption of corresponding figure, see [7] for the identification of morphological subtypes.

B. Discussions

We have proposed and developed a novel Independent Coordinates Method to quantify the regional curvature of the left ventricle from magnetic resonance imaging. We have tested the method in normal subjects and the patients with hypertrophic cardiomyopathy. These data have significant implications with respect to morphological subtype characterization and the clinical application of further function testing. The insight into the regional curvature of the left ventricle may have additional and potential incremental value over the conventional methods (i.e., ventricular wall thickness) to characterize hypertrophy type. Regional curvature of the left ventricle may influence the heart function and efficiency, as demonstrated in our prior study ([14]-[17]). Further, the gradient of curvature from epicardial to endocardial may have implication for myocardial fibrosis assessment. There are other potential applications such as the association of the LV curvature patterns to genetic mutations [7] and the relationship to the risk markers for sudden cardiac death in HCM patients.

We have shown using the ICM method, it is feasible to draw the curve of endocardium and epicardium. However, its clinical significance is uncertain as the subtypes can be easily assessed by visual in echo and MRI, even with patients motion. Nevertheless, we know there is intrinsic abnormality of regional contractile function in HCM that is not apparent on echo but require sensitive techniques like MR tagging ([11]-[13]). In our prior work ([14]-[17]), we have been able to assign functional meaning to local endocardial curvature, which appears to behave with the same periodicity and excursion as local strain and strain rate, and have created maps of normals and patients with LGE-determined infarcts. We believe the value here is that registration and curve generation in HCM yields local curvature information - endocardial or a derivative of endo and epi - can similarly unveil local contractile function.

Further, a recent study [18] shows there are regional of normal strain in the endocardial later and impaired strain in the epicardial regions. Perhaps, epi- and endocardial curvature analysis (which we can more efficiently calculate and analyse from unprocessed CMR cine images) can also shed light on such local heterogeneous function.

It is hope such a method can be used to track HCM serially to assess for progress of disease in a more sensitive manner than echo. At the very least, the epi and endo borders facilitate automatic display of myocardial thickness over time. While we not do treat HCM according to wall motion on echo, this paradigm may shift if we can find a truly sensitive method to characterize wall function and contractility. We know that hemodynamics and cardiac output can vary acutely with interventions in HCM. Are there concomitant changes in local myocardial function (which is a function of myocardial contractility and border conditions influenced by hemodynamic parameters)? We cannot routinely evaluate this as echo wall motion visualization is neither sensitive nor amenable to mathematical quantification. A modelled curvature-based method can potentially help here. Naturally, this shall require validation at some point in time.

Last, the difference between HCM and athletes heart is a clinical dilemma, and we think about analysing these cohorts using curvature based imaging.

V. CONCLUSIONS

ICM method to quantify regional curvature of the left ventricle from magnetic resonance imaging are feasible in normal subjects and those with hypertrophy cardiomyopathy, which may serve as a novel approach to depict local shape

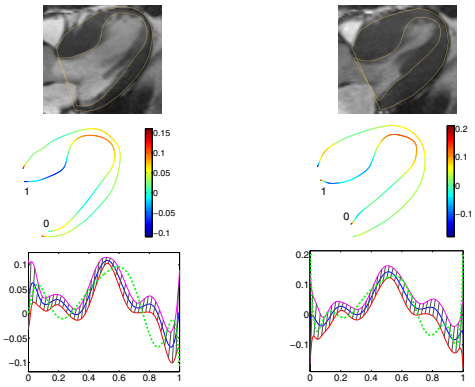

Fig. 5. Reverse curvature septum hypertrophic cardiomyopathy in a 29-year-old man.

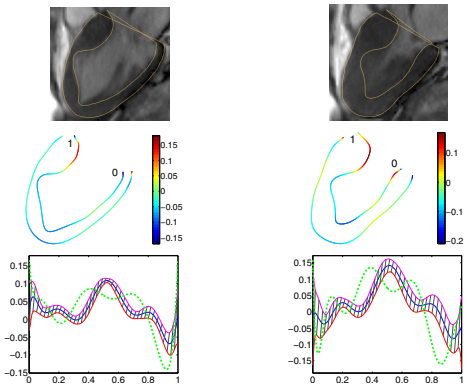

Fig. 6. Sigmoid septum hypertrophic cardiomyopathy in a 60-year-old woman.

of the left ventricle and to assess the morphological subtype in clinical practice.

ACKNOWLEDGMENT

This research is supported by the National Research Foundation (NMRC/EDG/1037/2011), Singapore under its Cooperative Basic Research Grant, the SingHealth Foundation (SHF/FG453P/2011) and (SHF/FG503P/2012), Singapore under its Translational Research Grant and administered by the SingHealth, the Goh Cardiovascular Research Grant (Duke-NUS-GCR/2013/0009), NHCS Centre Grant Seed Funding (NHCS-CGSF/2014/003), and Singapore-China Joint Research Programme (1215c013).

REFERENCES

[1] J.C. Kovacic, and D. Muller, "Hypertrophic cardiomyopathy: state-of-the-art review, with focus on the management of outflow obstruction," Intern. Med. J., vol. 33, pp. 521–529, Nov. 2003.

[2] P. Elliott, and W.J. McKenna, "Hypertrophic cardiomyopathy," Lancet, vol. 363, pp. 1881–1891, Jun. 2004.

[3] S.E. Hughes, "The pathology of hypertrophic cardiomyopathy," Histopathology, vol. 44, pp. 412–427, May 2004.

[4] E. Wigle, "The diagnosis of hypertrophic cardiomyopathy," Heart, vol. 86, pp. 709–714, Dec. 2001.

[5] M.W. Hansen, and N. Merchant, "MRI of hypertrophic cardiomyopathy: part I, MRI appearances," AJR. Am. J. Roentgenol., vol. 189, pp. 1335–1343, Dec. 2007.

[6] B.J. Maron BJ, M.S. Maron, C. Semsarian, "Genetics of hypertrophic cardiomyopathy after 20 years: clinical perspectives," J Am Coll Cardiol, vol 60, pp. :705C-715, Aug. 2012.

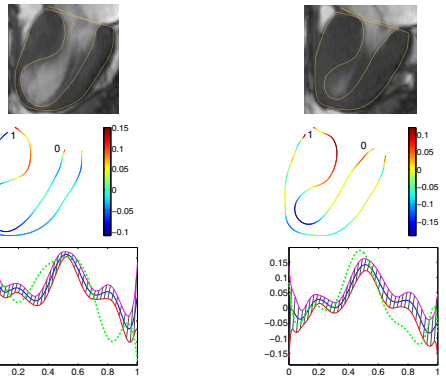

Fig. 7. Sigmoid septum hypertrophic cardiomyopathy in a 67-year-old woman.

[7] I.S. Syed, S.R. Ommen, J.F. Breen, and A.J. Tajik, "Hypertrophic Cardiomyopathy: Identification of Morphological Subtypes by E-chocardiography and Cardiac Magnetic Resonance Imaging," J. Am. Coll. Cardiol. Img., vol. 1, pp. 377–379, May 2008.

[8] T. Lewiner, J. Gomes, H. Lopes, and M. Craizer, "Curvature and torsion estimators based on parametric curve fitting," Computers and Graphics, vol. 29, pp. 641–655, Oct. 2005.

[9] A. Belyaev, "Plane and space curves, curvature, curvature-based features," (http://www.mpi-inf.mpg.de/ ag4-gm/handouts/).

[10] Y. An, C. Shao, X.L. Wang, and Z.H. Li, "Geometric properties estimation from discrete curves using discrete derivatives," Computers and Graphics, vol. 35, pp. 916–930, Feb. 2011.

[11] S.J. Dong, J.H. MacGregor, A.P. Crawley, E. McVeigh, I. Belenkie, E.R. Smith, J.V. Tyberg, R. Beyar, "Left ventricular wall thickness and regional systolic function in patients with hypertrophic cardiomyopathy. A three-dimensional tagged magnetic resonance imaging study," Circulation, vol. 90, pp. 1200–1209, 1994.

[12] Y. Mishiro, T. Oki, A. Iuchi, T. Tabata, H. Yamada, M. Abe, Y. Onose, S. Ito, H. Nishitani, M. Harada, Y. Taoka, "Regional left ventricular myocardial contraction abnormalities and asynchrony in patients with hypertrophic cardiomyopathy evaluated by magnetic resonance spatial modulation of magnetization myocardial tagging," Jpn Circ J, vol. 63, pp. 442–446, 1999.

[13] D.B. Ennis, F.H. Epstein, P. Kellman, L. Fananapazir, E.R. McVeigh, A.E. Arai, "Assessment of regional systolic and diastolic dysfunction in familial hypertrophic cardiomyopathy using MR tagging," Magn Reson Med, vol. 50, pp. 638–642, 2003.

[14] L. Zhong, Y. Su, S.Y. Yeo, R.S. Tan, "Ghista DN, Kassab G. Left ventricular regional wall curvature and wall stress in patients with ischemic dilated cardiomyopathy," Am J Physiology Heart Circ Physiol, vol. 3, pp. H573–H584, 2009.

[15] L. Zhong, Y. Su, L. Gobeawan, S. Sola, R.S. Tan, J.L. Navia, D.N. Ghista, T. Chua, J. Guccione, G.S. Kassab, "Impact of surgical ventricular restoration on ventricular shape, wall stress and function in heart failure patients," Am J Physiology Heart Circ Physiol, vol. 5, H1653–H1660, 2011.

[16] L. Zhong, L. Gobeawan, Y. Su, J.L. Tan, T. Chua, R.S. Tan, G. Kassab, "Right ventricular regional wall curvedness and area strain in patients with repaired Tetralogy of Fallot," Am J Physiology Heart Circ Physiol, vol. 6, H1306–H1316, 2012.

[17] Y. Su, L. Zhong, C.W. Lim, D.N. Ghista, T. Chua, R.S. Tan, "A geometrical approach for evaluating left ventricular remodeling in myocardial infarct patients," Comput Meth Prog Bio, vol. 108, pp. 500–510, 2012.

[18] H.A. Anthony, Gauri S. Tilak, Li-Yueh Hsu, Andrew E. Arai, "Heterogeneity of Intramural Function in Hypertrophic Cardiomyopathy. Mechanistic Insights From MRI Late Gadolinium Enhancement and High-Resolution Displacement Encoding With Stimulated Echoes Strain Maps," Circulation: Cardiovascular Imaging, vol. 4, pp. 425–434, 2011.